Journal of Molecular and Cellular Cardiology 62 (2013) 24–35

Contents lists available at SciVerse ScienceDirect

Journal of Molecular and Cellular Cardiology

journal homepage: www.elsevier.com/locate/yjmcc

Original article

Temporal dynamics of cardiac immune cell accumulation following acute myocardial infarction

Xiaoxiang Yan [a], Atsushi Anzai [a], Yoshinori Katsumata [a], Tomohiro Matsuhashi [a], Kentaro Ito [a], Jin Endo [a], Tsunehisa Yamamoto [a], Akiko Takeshima [a], Ken Shinmura [b], Weifeng Shen [c], Keiichi Fukuda [a], Motoaki Sano [a,d,*]

[a] Department of Cardiology, Keio University School of Medicine, Tokyo, Japan
[b] Department of Geriatric Medicine, Keio University School of Medicine, Tokyo, Japan
[c] Department of Cardiology, Ruijin Hospital, Shanghai Jiaotong University School of Medicine, Shanghai, China
[d] Precursory Research for Embryonic Science and Technology (PRESTO), Japan Science and Technology Agency, Tokyo, Japan

ARTICLE INFO

Article history:
Received 28 November 2012
Received in revised form 20 April 2013
Accepted 24 April 2013
Available online 2 May 2013

Keywords:
Myocardial infarction
Immune response
Macrophage polarity
Flow cytometry
Reperfusion therapy

ABSTRACT

Acute myocardial infarction (MI) causes sterile inflammation, which is characterized by recruitment and activation of innate and adaptive immune system cells. Here we delineate the temporal dynamics of immune cell accumulation following MI by flow cytometry. Neutrophils increased immediately to a peak at 3 days post-MI. Macrophages were numerically the predominant cells infiltrating the infarcted myocardium, increasing in number over the first week post-MI. Macrophages are functionally heterogeneous, whereby the first responders exhibit high expression levels of proinflammatory mediators, while the late responders express high levels of the anti-inflammatory cytokine IL-10; these macrophages can be classified into M_1 and M_2 macrophages, respectively, based on surface-marker expression. M_1 macrophages dominated at 1–3 days post-MI, whereas M_2 macrophages represented the predominant macrophage subset after 5 days. The M_2 macrophages expressed high levels of reparative genes in addition to proinflammatory genes to the same levels as in M_1 macrophages. The predominant subset of dendritic cells (DCs) was myeloid DC, which peaked in number on day 7. Th1 and regulatory T cells were the predominant subsets of $CD4^+$ T cells, whereas Th2 and Th17 cells were minor populations. $CD8^+$ T cells, γδT cells, B cells, natural killer (NK) cells and NKT cells peaked on day 7 post-MI. Timely reperfusion reduced the total number of leukocytes accumulated in the post-MI period, shifting the peak of innate immune response towards earlier and blunting the wave of adaptive immune response. In conclusion, these results provide important knowledge necessary for developing successful immunomodulatory therapies.

1. Introduction

Despite the introduction of current gold-standard cardioprotective therapies including β-blockers, renin–angiotensin–aldosterone system antagonists, anti-platelet agents, and statins, prognosis remains poor in post-MI patients, who often display adverse left ventricular (LV) remodeling after MI [1]. LV remodeling leads to congestive heart failure and is a main determinant of morbidity and mortality after MI [2]. At the present time, therapeutic options to prevent LV remodeling are limited.

MI causes sterile inflammation, which is characterized by the recruitment and activation of immune cells of the innate and adaptive immune systems. These cells may have a cell type-specific function in the time course after MI that involves clearance of dead tissues, the reparative response, and adverse remodeling [3–9]. Therefore, immunomodulatory therapies may harbor a promising potential for accelerating cardiac repair and ameliorating LV remodeling after MI. To develop optimal immunomodulatory therapies, it is mandatory to understand the temporal dynamics of immune cell accumulation following MI. In addition, reperfusion therapy is sure to change the temporal dynamics of post-MI immune responses. However, previous such studies are few in number and are focused on either one cell type only or semi-quantifying the immune cell accumulation by immunohistochemistry. A comprehensive characterization of the phenotype of immune cells in the infarct area is lacking and the effect of reperfusion therapy on the immune response remains unclear.

Available techniques for isolating cardiac immune cells remain problematic because heart is a solid and non-immune organ. In the

Abbreviations: ASC, Pycard; DC, Dendritic cell; DAMPs, Damage-associated molecular patterns; IR, Ischemia–reperfusion; Jmjd3, Jumonji domain containing 3; Klf4, Kruppel-like factor 4; LV, Left ventricular; Treg, Regulatory T cell.

* Corresponding author at: Department of Cardiology, Keio University School of Medicine, 35 Shinanomachi, Shinjuku-ku, Tokyo 160-8582, Japan. Tel.: +81 3 5363 3874; fax: +81 3 5363 3875.
E-mail address: msano@a8.keio.jp (M. Sano).

0022-2828/$ – see front matter © 2013 Elsevier Ltd. All rights reserved.
http://dx.doi.org/10.1016/j.yjmcc.2013.04.023

present study, we provided the methods how to characterize immune cells in the infarcted myocardium after MI. We then comprehensively investigated the temporal dynamics of immune cell accumulation following MI by flow cytometry and determined the impact of reperfusion therapy on the post-MI immune response.

2. Methods

2.1. Mice

C57BL6/J mice (20 to 25 g, male, 10–12 weeks; Nihon CLEA, Tokyo, Japan) were used in this study. This study conforms to the Guide for the Care and Use of Laboratory Animals published by the US National Institutes of Health (NIH publication no. 85-23, revised 1996) and was approved by the Institutional Animal Care and Use Committee at the Keio University School of Medicine.

2.2. Induction of MI and IR models

Mice were subjected to a permanent (MI) or transient (IR) ligation of the left anterior descending artery or to a sham operation without ligation, as described previously [3,10]. In brief, mice were lightly anesthetized with diethyl ether, intubated, and then fully anesthetized with 1.0–1.5% isoflurane gas while being mechanically ventilated with a rodent respirator. The chest cavity was opened via left thoracotomy to expose the heart, such that the left anterior descending coronary (LAD) could be visualized by the microscope and be permanently ligated with a 7–0 silk suture at the site of its emergence from the left atrium. Complete occlusion of the vessel was confirmed by the presence of myocardial blanching in the perfusion bed. Mice that died within 24 h after surgery were excluded from the experiment. Sham-operated animals underwent the same procedure without coronary artery ligation. Large infarctions were induced by proximal ligation of the LAD at the site of its emergence from the left atrium, and moderate infarctions were induced by ligation of middle parts of LAD. To induce IR, a slipknot was made around the left anterior descending coronary artery against PE10 tubing with a 7–0 silk suture. After 45 min of ligation, the ligature was released to allow reperfusion. In the immune cell infiltration experiments, the sham operation was done and the animals sacrificed at different time points. We also proved in a separate experiment that macrophage, T cell, and neutrophil numbers in the heart did not change over the time course after sham operations.

2.3. Infarct size evaluation and morphometric analysis

To evaluate the infarct size after MI, hearts were removed and frozen at −80 °C; however, for IR model, the ligature around the coronary artery was retied, and 1 ml of 2% Evans Blue dye was injected into the apex of the heart. The frozen heart was cut transversely into 1-mm-thick slices using a Mouse Heart Slicer Matrix, and stained with 2% TTC in PBS (pH 7.4) for 20 min in a 37 °C water bath. After fixation for 4–6 h in 10% neutral buffered formaldehyde, both sides of each slice were photographed. The viable myocardium stained brick red, and infarct tissues appeared pale white. Infarct and LV area were measured by automated planimetry using ImageJ software (version 1.43u, National Institutes of Health), with the infarct size expressed as a percentage of the total LV area. To evaluate the cardiac remodeling at 28 days after MI, heart tissue was fixed in formalin, embedded in paraffin, and cut into 5-μm-thick sections. Azan staining was performed on paraffin-embedded sections to determine the morphological effects and extent of cardiac fibrosis. The area of myocardial fibrosis in left ventricular was measured and analyzed using analysis software (BZ image analyzer II; Keyence).

2.4. Cell preparation for flow cytometry

At each time point, the mice were deeply anesthetized and intracardially perfused with 40 ml of ice-cold PBS to exclude blood cells. The heart was dissected, minced with fine scissors, and enzymatically digested with a cocktail of type II collagenase (Worthington Biochemical Corporation, Lakewood, NJ), elastase (Worthington Biochemical Corporation), and DNase I (Sigma, St. Louis, MO) for 1.5 h at 37 °C with gentle agitation. After digestion, the tissue was triturated and passed through a 70-μm cell strainer. Leukocyte-enriched fractions were isolated by 37–70% Percoll (GE Healthcare) density gradient centrifugation as described elsewhere [11]. Cells were removed from the interface and washed with RPMI-1640 cell culture medium for further analysis. Spleens were removed, homogenized, and then passed through a 70-μm nylon mesh in PBS. After addition of red blood cell lysis buffer (eBioscience) to exclude erythrocytes, the single cell suspension in PBS was refiltered through a 70-μm nylon mesh to remove connective tissue.

2.5. Flow cytometric analysis

Cell suspensions isolated from spleen and leukocyte-enriched fractions from heart were analyzed by flow cytometry. To block nonspecific binding of antibodies to Fcγ receptors, isolated cells were first incubated with anti-CD16/32 antibody (2.4G2, BD Bioscience) at 4 °C for 5 min. Subsequently, the cells were stained with a mixture of antibodies at 4 °C for 20 min. Results were expressed as cell number per heart. Flow cytometric analysis and sorting were performed on a FACSAriaI and III instrument (BD Biosciences) and analyzed using FlowJo software (Tree Star).

2.6. Statistical analysis

Values are presented as mean ± SEM. Data among multiple groups were compared using either the Kruskall–Wallis test with Dunn's multiple comparison test or two-way ANOVA followed by Tukey's post hoc analysis, as appropriate. A value of $P < 0.05$ was considered statistically significant. Statistical analysis was performed with GraphPad Prism 5.0 (GraphPad Prism Software Inc., San Diego, CA, USA) and SPSS 15.0 for Windows (SPSS, Inc., Chicago, IL, USA).

3. Results

3.1. Immune cell definition by surface markers

After a 70%–37% Percoll gradient centrifugation, $CD45^+$ leukocytes were enriched either within the 37%/70% interface or the 70% Percoll solution (Supplementary Fig. 1). Single cell suspensions from freshly obtained leukocyte-enriched fractions were analyzed for CD11b and CD45 expression using flow cytometry (Fig. 1A). $CD45^+CD11b^+$ myeloid cells were divided into $F4/80^+$ macrophages and $Ly\text{-}6G^+$ neutrophils, with the $F4/80^+$ macrophages further divided based on M_1 (classically activated macrophages, $CD206^{low}$) and M_2 (alternatively activated macrophages, $CD206^{high}$) polarity. $CD45^+CD11b^{low}$ cells comprised T cells, B cells, natural killer cells (NK cells), and natural killer T (NKT) cells. The T cells were further divided into $CD4^+$-αßT cells, $CD8^+$-αßT cells, and γδT cells, while NK cells and NKT cells were defined as $CD45^+CD11b^{low}NK1.1^+CD3^-$ and $CD45^+CD11b^{low}NK1.1^+CD3^+$, respectively. The prominent subsets of $CD45^+CD11c^+MHC\text{-}II^+$ dendritic cells (DCs) were $CD11b^+$ myeloid DCs (Fig. 1B).

3.2. Temporal dynamics of the cellular infiltrate after permanent myocardial infarction

We initially performed a detailed temporal analysis of cellular infiltrate dynamics in the post-MI heart. The total number of infiltrating $CD45^+$ leukocytes gradually increased after MI to a peak on day 7

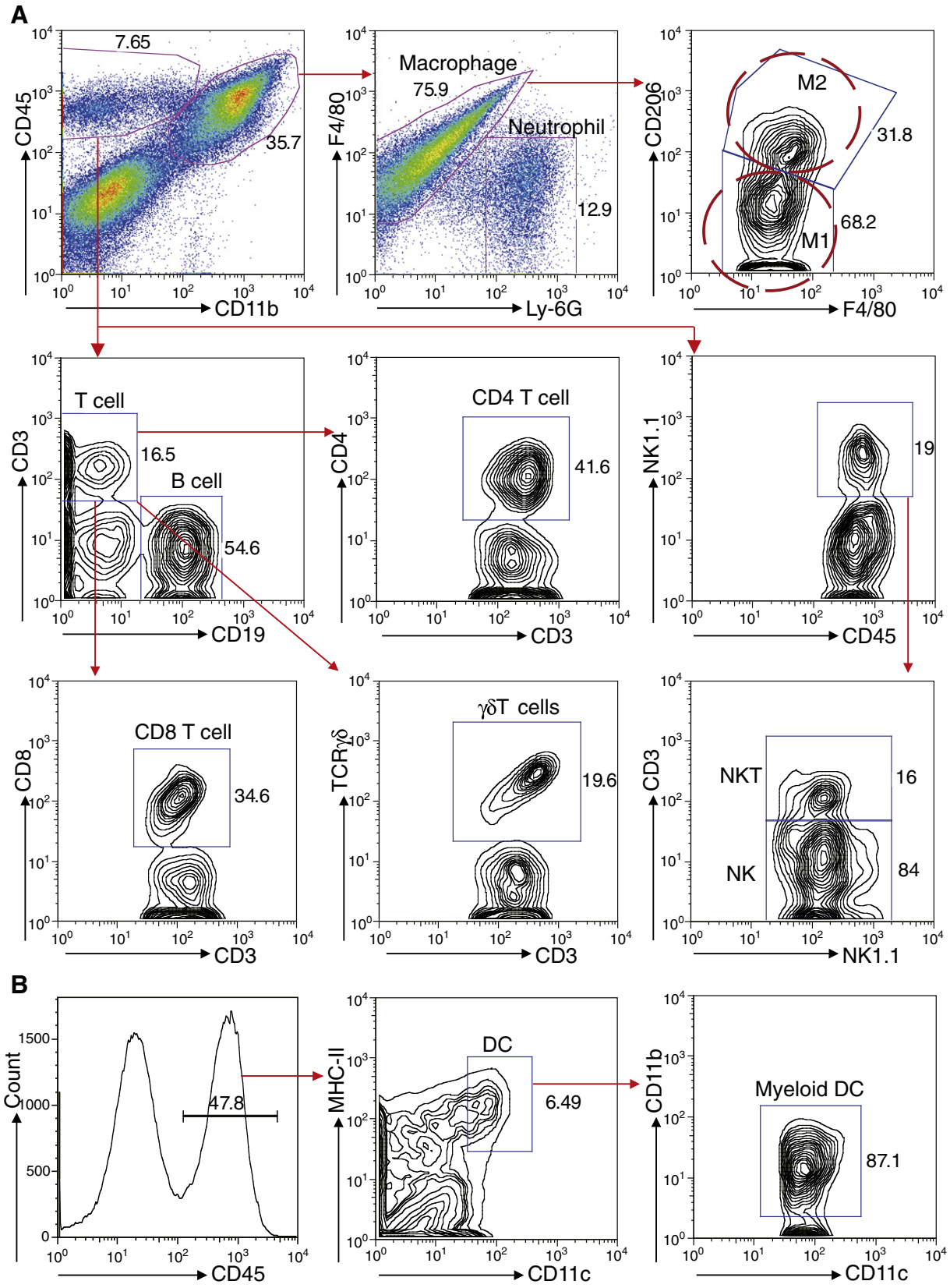

Fig. 1. Gating strategy for infiltrating immune cells in the infarcted heart. (A) Populations collected from 37/70% and 70% Percoll fractions were stained for CD45 and CD11b, allowing the identification of 3 different populations: $CD45^{+}CD11b^{+}$ myeloid cells, $CD45^{+}CD11b^{low}$ cells, and $CD45^{-}CD11b^{low}$ non-leukocytes. The $CD45^{+}CD11b^{+}$ population contained $CD11b^{+}F4/80^{+}$ macrophages and $CD11b^{+}Ly\text{-}6G^{+}$ neutrophils. Macrophages were further divided into M_1 and M_2 macrophages based on the expression of CD206. The $CD45^{+}CD11b^{low}$ population was gated into T cells (including $CD4^{+}$, $CD8^{+}$, and γδT cells), B cells, natural killer cells (NK cells), and NKT cells with staining for CD3, CD19, CD4, CD8, TCRγδ, and NK1.1. (B) A leukocyte-enriched fraction was stained for CD45, CD11c, MHC-II, and CD11b. Dendritic cells (DCs) were defined as $CD45^{+}CD11c^{+}MHC\text{-}II^{+}$ cells; most were $CD11b^{+}$ myeloid DC.

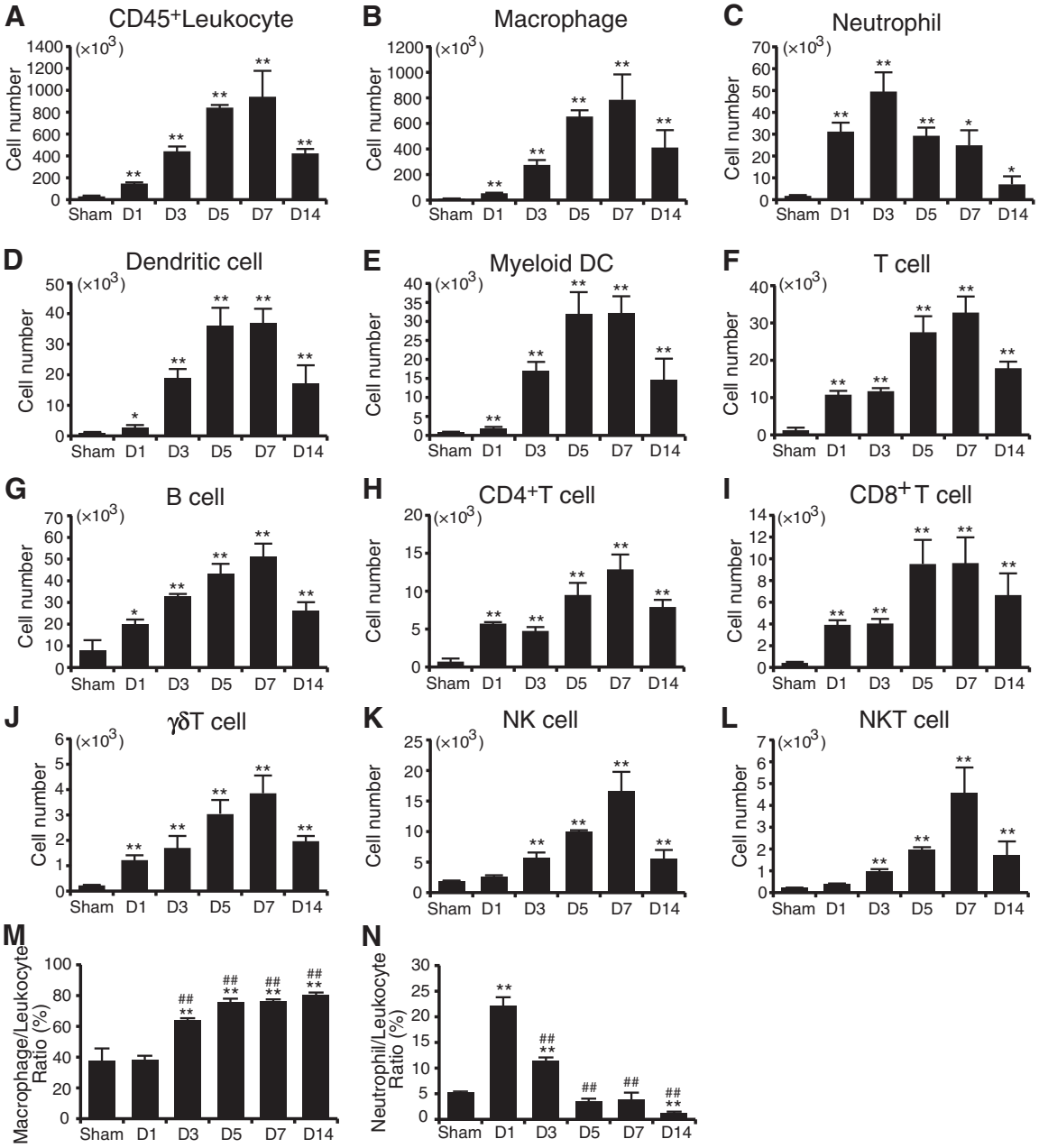

Fig. 2. Quantification and characterization of temporal dynamics of the immune response in the permanent MI heart. (A through L) Quantities represent absolute number of cells per heart (n = 4–7, each). $^{*}P < 0.05$, $^{**}P < 0.01$ vs. sham. (M, N) Percentages of macrophages (M) and neutrophils (N) in $CD45^+$ leukocytes infiltrated after MI (n = 4–7, each time point). $^{**}P < 0.01$ vs. sham, $^{\#\#}P < 0.01$ vs. day 1 post-MI. Data were analyzed by Kruskall–Wallis tests with Dunn's multiple comparison.

(Fig. 2). Neutrophils also accumulated in the infarcted heart, peaking at 3 days after MI and then notably, continuing to accumulate in the infarcted myocardium over 7–14 days after the MI onset. Numerically, macrophages were the predominant cells infiltrating the infarcted myocardium, and these cells showed a biphasic pattern of activation (Figs. 3A–E). M_1 macrophages dominated on 1 to 3 days post-MI, whereas M_2 macrophages increased more gradually and represented the predominant macrophage subset after 5 days post-MI. DC accumulation reached a maximum on day 5–7 after MI. Infiltrating $CD4^+$-αßT cells, $CD8^+$-αßT cells and γδT cells, and B cells started to increase gradually to a peak on day 7 after MI. NK cells and NKT cells started to increase on day 3 and peaked on day 7 after MI.

Immunohistochemical analysis at day 7 after permanent post-MI showed that $F4/80^+$ macrophages were located mostly in the infarct/border zone and to a much lesser extent in the remote area (Supplementary Fig. 2). The numbers of T lymphocytes are low in the infarct/border zone and could only sporadically observe in the remote area.

3.3. Biphasic pattern of macrophage activation defined by different surface marker expressions in the post-MI heart

When monocytes migrate from the circulation and extravasate through the endothelium, they differentiate into macrophages, which represent a spectrum of activated phenotypes with significant overlap in surface marker expression among the different macrophage subsets [12]. In the present study, we analyzed expression of the cell surface markers, CD206, Ly-6C, F4/80, and CD11b, to characterize two different functions of macrophages, namely M_1 macrophages and M_2 macrophages (Figs. 3A–F). We defined $CD206^{low}$, Ly-$6C^+$, and $CD11b^+F4/80^{low}$ expressors as M_1 macrophages, and these were the predominate macrophages in the early stages of post-MI healing. Cells showing

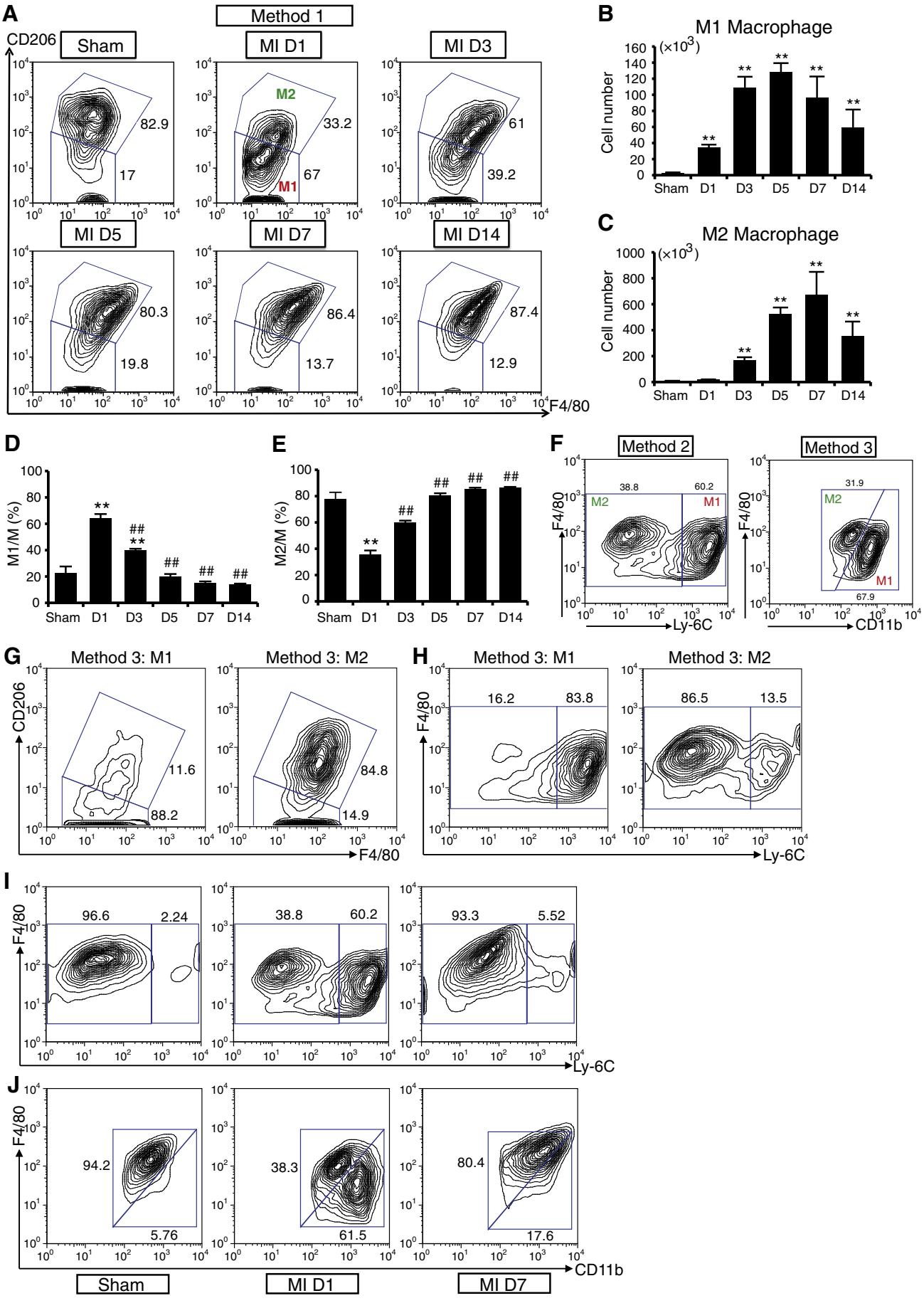
A
Method 1
CD206
Sham
MI D1
MI D3
MI D5
MI D7
MI D14
M2
M1
82.9
17
33.2
67
61
39.2
80.3
19.8
86.4
13.7
87.4
12.9
F4/80
B
M1 Macrophage
(×10^3)
Cell number
Sham D1 D3 D5 D7 D14
C
M2 Macrophage
(×10^3)
Cell number
Sham D1 D3 D5 D7 D14
D
M1/M (%)
Sham D1 D3 D5 D7 D14
E
M2/M (%)
Sham D1 D3 D5 D7 D14
F
Method 2
Method 3
38.8
60.2
M2
M1
31.9
67.9
F4/80
Ly-6C
CD11b
G
Method 3: M1
Method 3: M2
CD206
11.6
88.2
84.8
14.9
F4/80
H
Method 3: M1
Method 3: M2
F4/80
16.2
83.8
86.5
13.5
Ly-6C
I
F4/80
96.6
2.24
38.8
60.2
93.3
5.52
Ly-6C
J
F4/80
94.2
5.76
38.3
61.5
80.4
17.6
CD11b
Sham
MI D1
MI D7

$CD206^{high}$, Ly-$6c^{-}$, and $CD11b^{low}F4/80^{high}$ expressions were defined as M_2 macrophages; these were the predominant cell type in sham-operated heart and increased in number at the later stage of post-MI healing.

We also compared different surface markers to identify M1 and M2 macrophages. Nearly 90% of $CD11b^{+}F4/80^{low}$ macrophages were $CD206^{low}$ M_1 macrophages, and 85% of $CD11b^{low}F4/80^{high}$ macrophages were $CD206^{high}$ M_2 macrophages. In addition, approximately 85% of $CD11b^{+}F4/80^{low}$ macrophages were Ly-$6C^{high}$ M_1 macrophages, and 86% of $CD11b^{low}F4/80^{high}$ macrophages were Ly-$6C^{low}$ M_2 macrophages (Figs. 3G–J). These results indicated that these different surface markers are comparable for the identification of M_1 and M_2 macrophage during post-MI healing.

3.4. Changes in the gene expression profile of sorted macrophages during the time course after MI

Next, we quantified specific gene expression profiles in the macrophages accumulated at the various stages of post-MI healing, and found dramatic changes in the sorted macrophage profiles according to the shift in macrophage phenotype and function (Fig. 4). First-responder macrophages exhibited higher expression levels of pro-inflammatory genes. Corresponding to the increased expression of Toll-like receptor (TLR)4 and TLR6, the expression levels of pro-inflammatory mediators such as IL-6, IL-1β, NOS2, IL-12a, and IL-23a, S100a8, and S100a9 were markedly upregulated in the first-responder macrophages in this study. NLRP3 inflammasome component ASC (gene name: Pycard) was also upregulated in the first-responder macrophages. By contrast, the late-responder macrophages expressed high levels of anti-inflammatory cytokine IL-10 (Figs. 4A–C, F and G).

In terms of chemokine receptors, the first-responder macrophages express high levels of CCR2, CCR7, and CXCR7, whereas the late-responding macrophages expressed high levels of CX3CR1. The co-stimulatory molecules CD80 and CD86 were differentially expressed; CD80 was predominantly expressed in the first-responder macrophages, and CD86 in the late responders (Figs. 4H–J).

Two adhesion molecules, CD11b (Itgam) and L-selectin, were also highly expressed in the first-responder macrophages, whereas transcription factors that regulate M_2 macrophage polarization, Jmjd3, Klf4, Stat3, and Pparγ, were highly expressed in the late responders and resident macrophages (Figs. 4D and K). The expression of MHC class II (MHC-II) enables macrophages to express antigens to $CD4^{+}$ T cells and also promotes adaptive immunity. Resident and late-responder macrophages exhibited high expression levels of MHC-II, whereas 70% of first-responder macrophages had low expression levels of MHC-II (Figs. 4L and M).

3.5. M_2 macrophages displayed mixed gene expression profile of both reparative and proinflammatory activities

M_1 ($CD206^{low}$) and M_2 ($CD206^{high}$) macrophages were separately isolated from hearts of mice 1 day and 7 days after MI. The defined M_1 macrophages expressed high levels of M_1 signature genes, such as TNF-α, IL-6, CCL2, and NOS2, with minimal expression levels of M_2 signature genes such as IL-10, arginase 1, and TGF-β. By contrast, M_2 macrophages expressed high levels of M_2 signature genes as well as the M_1 signature genes, with the latter at the same levels as in M_1 macrophages. These findings indicated that M_1 macrophages have an exclusively proinflammatory character, whereas M_2 macrophages possess both reparative and proinflammatory characters (Fig. 5).

3.6. Polarization of Th1 and Treg cells in the infarcted heart

$CD4^{+}$ naïve T cell can differentiate into Th1, Th2, Th17 and regulatory T cells (Treg) [9]. In this study, IL-12p35 was dramatically increased on day 1 post-MI (Fig. 6A), while expression of the Th1-related transcriptional factor TBX21 (Fig. 6B) and Th1 cytokine IFN-γ (Fig. 6C) in the infarcted myocardium increased gradually to a peak on days 7 and 14. Consistent with this, the number of infiltrating IFN-γ-producing $CD4^{+}$ cells increased gradually and peaked on days 7 and 14 (Figs. 6D and E). By contrast, there was no change in the expression levels of Th2-related transcriptional factor GATA3 (Fig. 6F) or the number of IL-4-producing $CD4^{+}$ cells after MI (Fig. 6G). Th1/Th2 imbalance towards Th1 was thus apparent in the infarcted myocardium.

As we previously reported, Th17 was not the major source of IL-17A (Fig. 6H) in the post-MI heart and most IL-17A-producing cells accumulated in the infarct were γδT cells [13].

The expression of regulatory T (Treg) cell lineage-specific transcription factor Foxp3 (Fig. 6I) and the numbers of $Foxp3^{+}$ Treg cells increased gradually over a week following MI (Fig. 6J). The expression levels of IL-10 in the infarct also increased gradually and peaked on day 7 after MI (Fig. 6K). The percentage of Treg in spleen did not change after MI, suggesting a specific recruitment of Treg to the infarcted hearts.

3.7. Temporal dynamics of immune response after MI are changed by timely reperfusion of occluded coronary arteries

To elucidate the effect of infarct size on immune cells infiltration, we created MI of varied sizes using the proximal and middle part of LAD ligation (Supplementary Fig. 3). On day 6 post-MI, echocardiographic examination revealed a markedly enlarged heart (LVEDD 5.96 ± 0.07 mm, n = 5) with reduced LV systolic function (FS 5.2 ± 1.01%, n = 5) after the LAD proximal ligation, whereas significantly less LV enlargement (LVEDD 4.51 ± 0.21 mm, n = 5) and significantly less severe LV dysfunction (FS 22.3 ± 1.7%) was apparent after the LAD middle ligation. In parallel with the infarct size, macrophages and T cells were significantly more abundant at 7 days post-MI in severe MI mice compared to moderate MI mice, suggesting that infarct size is the main determinant for the numerical dynamics of immune cells after MI with persistent total occlusion of the infarct artery.

Next, we investigated the impact of timely reperfusion on infarct size and post-MI remodeling together with immune response temporal dynamics after MI (Fig. 7 and Supplementary Fig. 4). The morphology of the infarct differed between persistent total occlusion of the infarct artery (LAD proximal) and timely reperfusion of occluded coronary arteries. The MI with persistent total occlusion of the infarct artery was transmural (Supplementary Fig. 4). By contrast, the reperfused MI affected primarily the epicardial layer while the endocardial layers were spared [14–18]. After reperfusion, the infarct size on day 4 post-MI was significantly less and the adverse remodeling on day 28 post-MI, measured by LV lumen dilatation and extent of

Fig. 3. Comparison of three methods defining the macrophage activation pattern in the post-MI heart. (A) Representative flow cytometric analysis of M_1 macrophages ($CD11b^{+}F4/80^{+}CD206^{-}$) and M_2 macrophages ($CD11b^{+}F4/80^{+}CD206^{+}$) (Method 1) in the post-MI heart. Cells were gated on $CD45^{+}CD11b^{+}F4/80^{+}$Ly-$6G^{-}$ macrophages for flow cytometry. (B–E) Time courses of changes in the M_1, M_2 macrophage (Method 1) absolute cell number (B and C) and their percentages relative to the total macrophage population (D and E) infiltrated into the infarcted heart. (n = 4–7, each). $^{**}P < 0.01$ vs. sham, $^{\#\#}P < 0.01$ vs. day 1 post-MI. Data were analyzed by Kruskall–Wallis tests with Dunn's multiple comparison. (F) Macrophages ($CD45^{+}CD11b^{+}F4/80^{+}$Ly-$6G^{-}$) were defined as M_1 and M_2 macrophages according to Ly-6C (Method 2) and CD11b expression (Method 3) levels. Data were obtained from at least five independent experiments. (G, H) Macrophages defined by method 3 were re-analyzed with CD206 (G, method 1) and Ly-6C (H, method 2) expression levels, with results revealing that these three methods are comparable for the identification of M_1 and M_2 macrophage in post-MI heart. Data represent four independent experiments. (I, J) Time courses of changes in biphasic macrophage activation defined by Ly-6C (Method 2) and CD11b (Method 3). Data represent four independent experiments.

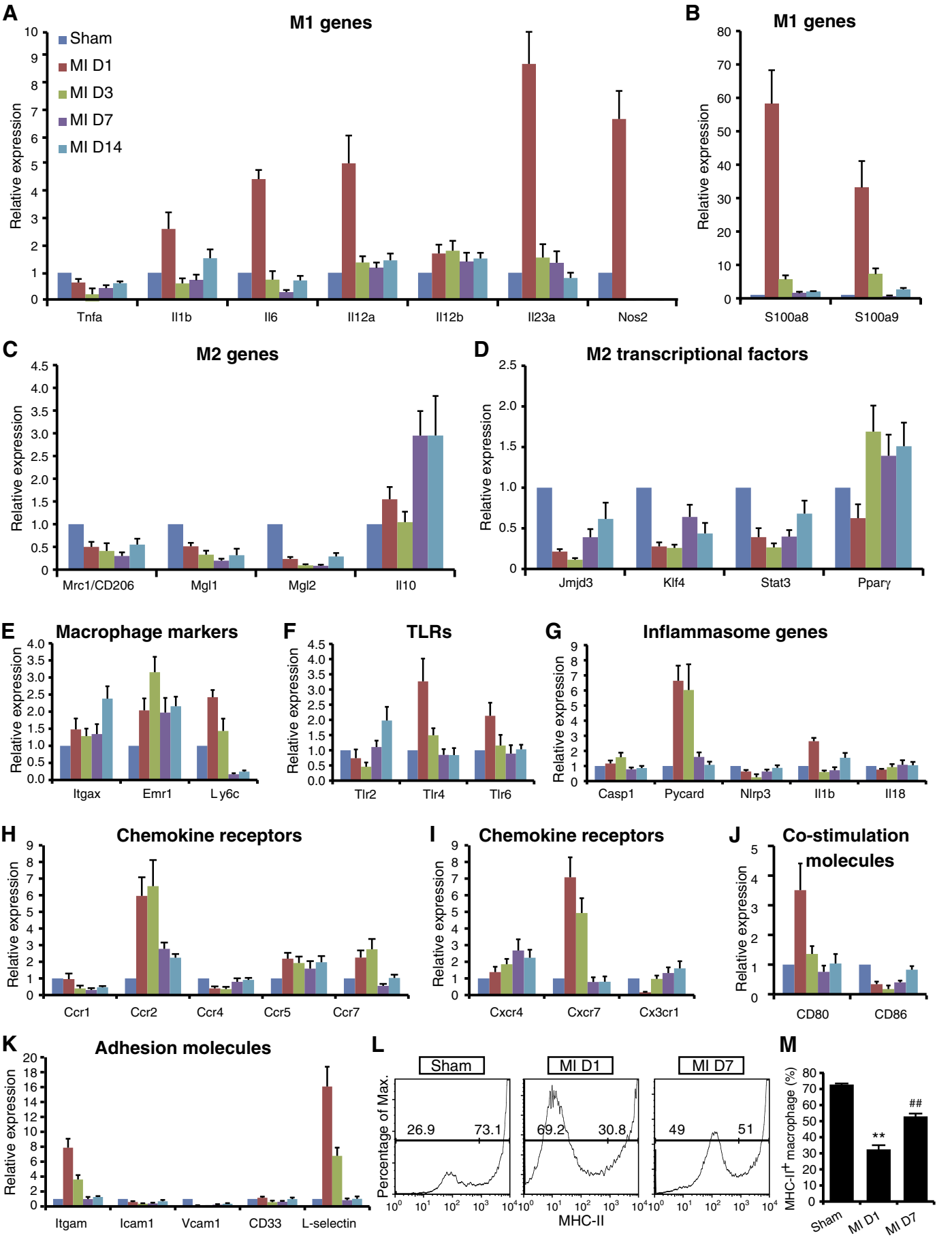
A
M1 genes
Sham
MI D1
MI D3
MI D7
MI D14
Relative expression
Tnfa
Il1b
Il6
Il12a
Il12b
Il23a
Nos2
B
M1 genes
Relative expression
S100a8
S100a9
C
M2 genes
Relative expression
Mrc1/CD206
Mgl1
Mgl2
Il10
D
M2 transcriptional factors
Relative expression
Jmjd3
Klf4
Stat3
Pparγ
E
Macrophage markers
Relative expression
Itgax
Emr1
Ly6c
F
TLRs
Relative expression
Tlr2
Tlr4
Tlr6
G
Inflammasome genes
Relative expression
Casp1
Pycard
Nlrp3
Il1b
Il18
H
Chemokine receptors
Relative expression
Ccr1
Ccr2
Ccr4
Ccr5
Ccr7
I
Chemokine receptors
Relative expression
Cxcr4
Cxcr7
Cx3cr1
J
Co-stimulation molecules
Relative expression
CD80
CD86
K
Adhesion molecules
Relative expression
Itgam
Icam1
Vcam1
CD33
L-selectin
L
Sham
MI D1
MI D7
Percentage of Max.
26.9
73.1
69.2
30.8
49
51
MHC-II
M
MHC-II+ macrophage (%)
**
##
Sham
MI D1
MI D7

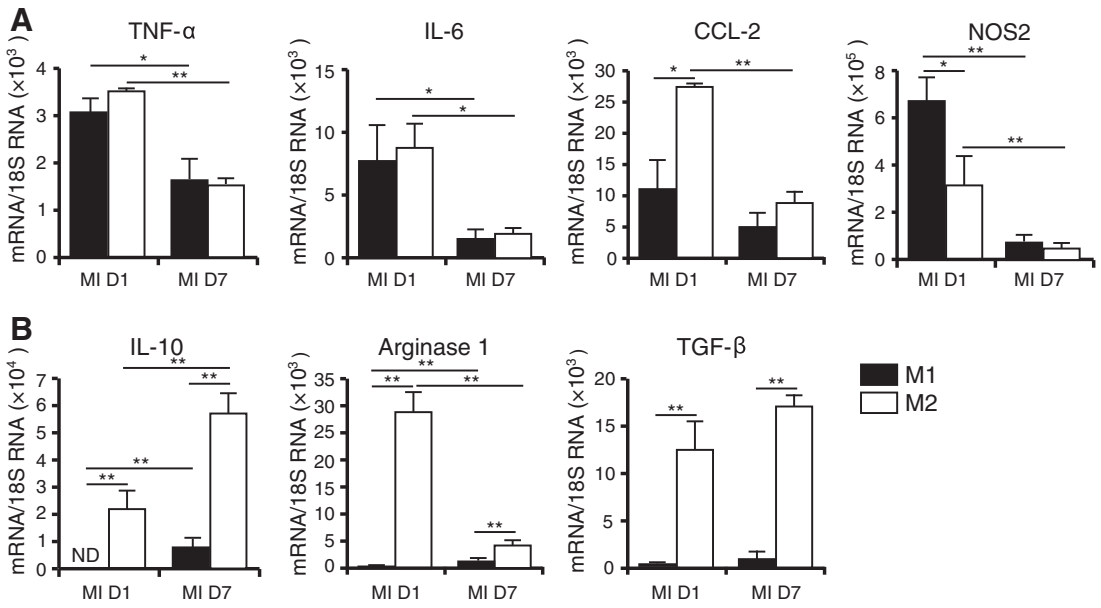

Fig. 5. M_2 macrophages displayed mixed gene expression profiles of both M_1 and M_2 macrophages. The mRNA expression levels of pro-inflammatory (A) and anti-inflammatory (B) genes were quantified in M_1 macrophages ($CD11b^+F4/80^+CD206^-$) and M_2 macrophages ($CD11b^+F4/80^+CD206^+$) sorted from heart on day 1 and day 7 post-MI (n = 5 or 6). $^*P < 0.05$, $^{**}P < 0.01$. Data were analyzed by two-way ANOVA followed by Tukey's post hoc analysis.

fibrosis, was significantly less than after MI, with persistent total occlusion of the infarct artery.

The total number of leukocytes reached a maximum level on day 7 after MI with persistent total occlusion of the infarct artery, while timely reperfusion of occluded coronary arteries shifted this peak towards day 3. In addition, leukocyte accumulation persisted until day 14 after MI with persistent total occlusion of the infarct artery; however, timely reperfusion of the occluded coronary arteries reduced the total number of leukocytes accumulating in the infarcted myocardium to less than 20%, and most had disappeared on day 7 after MI. This treatment thus temporally shifted the innate and adaptive immune response dynamics to an earlier point post-MI; specifically, the peak of neutrophil infiltration was shifted from day 3 to day 1, while the peak of macrophage infiltration shifted from day 7 to day 3. In terms of the adaptive immune response, timely reperfusion also shifted the peak of DC, $CD4^+$ T cell, B cell, γδT cell, NK cell, and NKT cell accumulation from day 7 to day 3 and blunted the wave of these adaptive immune responses. There was a peak delay of several days following the adaptive immune response in the setting of MI with persistent total occlusion of the infarct artery, but this was shortened between the innate and adaptive immune responses by the reperfusion. These findings indicated that timely reperfusion changed the course and the content of immune cells influx and evanescence in the infarcted myocardium.

4. Discussion

The present study provides a precise and comprehensive analysis of the temporal dynamics of immune cell infiltration after MI by flow cytometry. Peripheral blood contains mostly monocytes, and when monocytes migrate from the circulation and extravasate through the endothelium, they become macrophages. Nahrendorf and their colleagues demonstrated that heart tissue under steady-state conditions contains mostly $F4/80^{high}$ macrophages, while ischemic myocardium contains predominantly $F4/80^{low}$ monocytes, but not $F4/80^{high}$ macrophages, at least during the first week after coronary occlusion [4]. Our definition of macrophage populations by flow cytometry is $CD45^+/CD11b^+/F4/80^+/Ly6G^-$ cells. Fluorescence intensities for F4/80 signals on our defined macrophages were comparable between sham-operated hearts and hearts at days 1, 3, 5, and 7, and at 14 days post-MI. Furthermore, the expression levels of F4/80, also known as Emr1, in isolated macrophages started to increase at day 1 post-MI and remained elevated until day 14, suggesting that monocytes may commit to macrophages as early as day 1 after MI. Monocytes and macrophages shared cell surface markers depending on functional diversity, thus it is difficult to distinguish between monocytes and macrophages by cell surface markers. In other words, macrophages can be regarded as "activated monocytes" and the activation probably occurs when monocytes extravasate through the endothelium.

One of the major findings of this paper is the change over time following MI in macrophage gene expression profiles. These dynamic changes in gene expression might explain why macrophages can accomplish diverse and seemingly contrasting functions. The first-responder macrophages expressed high levels of pro-inflammatory mediators, whereas the late responders expressed high levels of anti-inflammatory cytokine IL-10. S100A8 and S100A9 produced by macrophages are critical for recruiting inflammatory monocytes and their subsequent differentiation into M_1 macrophages [19–21]. Interestingly, S100A8 and S100A9 expressions were also highly elevated in the first-responder macrophages. Costimulatory molecules CD80/CD86 can regulate inflammation in both the innate and adaptive immune responses. For instance, neutrophils expressing CD28 activate macrophages in a contact-dependent manner via engagement of CD80/CD86 [22]. We found that the macrophage expression of CD80 and CD86

Fig. 4. Time course changes in gene expression profile in the macrophages sorted from post-MI heart. $CD11b^+F4/80^+Ly\text{-}6G^-$ macrophages were sorted from the post-MI heart at the indicated time points, and quantitative RT-PCR was employed to measure the M_1 (A, B), M_2 (C) signature genes and M_2-related transcriptional factors (D). mRNA levels of macrophage markers (E), Toll-like receptors (F), NLRP3 inflammasome genes (G), chemokine receptors (H, I), co-stimulators (J), and adhesion molecules (K) were also quantified by qPCR. n = 4–6 for each time point. (L, M) MHC-II expression in cardiac macrophages at the indicated time points. Cells were gated on $CD45^+CD11b^+F4/80^+Ly\text{-}6G^-$ macrophages. Data are representative of five experiments. $^{**}P < 0.01$ vs. sham, $^{\#\#}P < 0.01$ vs. MI D1 (Kruskall–Wallis tests with Dunn's multiple comparison).

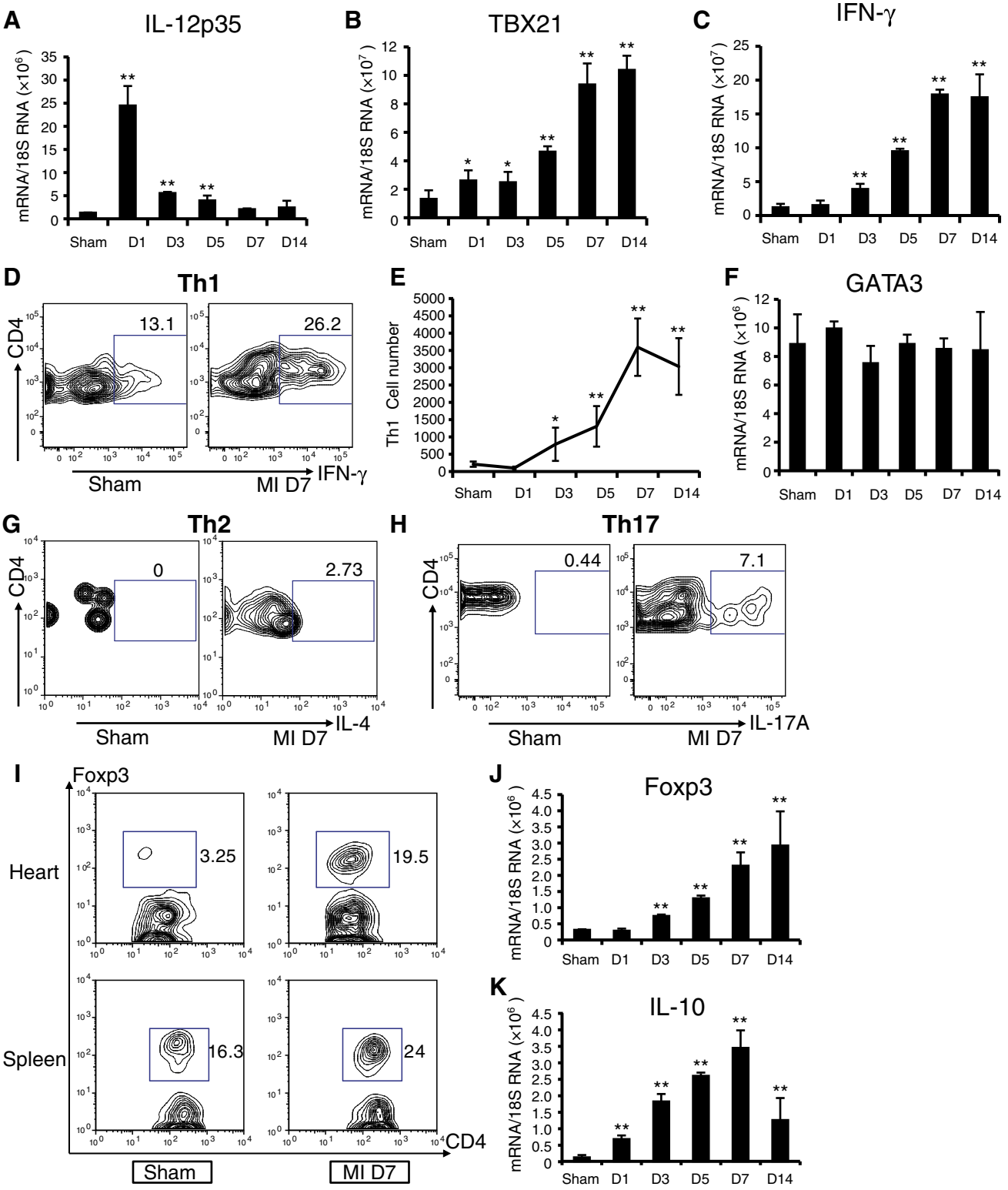

Fig. 6. Polarization of Th1 and Treg cells in the infarcted heart. (A–C) Time course of changes in the mRNA expression of IL-12p35 (A), TBX21 (B), and IFN-γ (C) in the heart tissue after MI. The levels of each transcript were normalized to 18S (n = 4–6 each). $^{*}P < 0.05$, $^{**}P < 0.01$ vs. sham. (D) Intracellular IFN-γ staining combined with surface markers was performed on the enriched leukocytes prepared from heart on day 7 post-MI. Cells were gated on $CD45^{+}CD11b^{-}CD3^{+}CD4^{+}$ cells. Data are representative of four independent experiments. (E) Time course of change in numbers of infiltrating $CD4^{+}IFN\text{-}\gamma^{+}$ (Th1) cells in the infarcted heart (n = 4–6 each). $^{*}P < 0.05$, $^{**}P < 0.01$ vs. sham heart. (F) mRNA expression of GATA3 in the heart tissue after MI. The levels of each transcript were normalized to 18S (n = 4–6 each). Intracellular IL-4 (G), IL-17A (H) and Foxp3 (I) staining combined with surface markers was performed on the enriched leukocytes prepared from heart or spleen on day 7 post-MI. Cells were gated on $CD45^{+}CD11b^{-}CD3^{+}CD4^{+}$ cells. Data are representative of at least four independent experiments. (J, K) Time course of changes in the mRNA expression of Foxp3 (J) and IL-10 (K) in the heart tissue after MI. The levels of each transcript were normalized to 18S (n = 4–6 each). $^{**}P < 0.01$ vs. sham. Data in A, B, C, E, F, J and K were analyzed by Kruskall–Wallis tests with Dunn's multiple comparison.

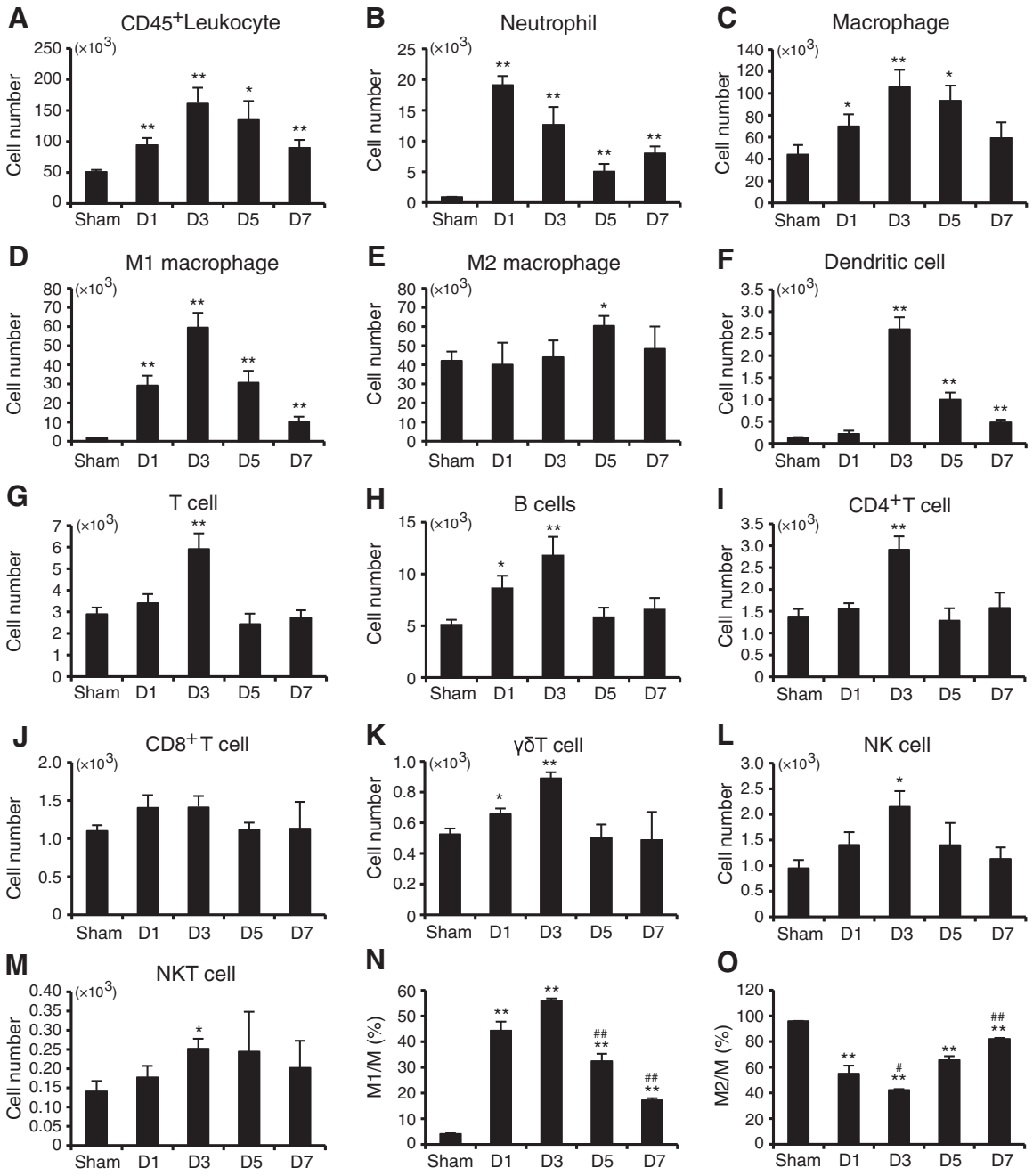

Fig. 7. Quantification and characterization of temporal dynamics of the immune response in the heart after IR injury. (A through M) Time courses of changes in the absolute immune cell number infiltrated into the heart after IR injury (n = 4–6, each). $^{*}P < 0.05$, $^{**}P < 0.01$ vs. sham. (N, O) Percentages of M_1 macrophages ($CD11b^{+}F4/80^{+}CD206^{-}$) and M_2 macrophages ($CD11b^{+}F4/80^{+}CD206^{+}$) among total macrophages from heart after cardiac IR injury (n = 4–6, each). $^{**}P < 0.01$ vs. sham, $^{\#}P < 0.05$, $^{\#\#}P < 0.01$ vs. day 1 after IR. Data in A, B, C, E, F, J and K were analyzed by Kruskall–Wallis tests with Dunn's multiple comparison.

was differentially regulated in the time course after MI, with the first responders showing an increased CD80 expression and downregulated CD86 expression. Our results are consistent with a previous report of upregulation of CD80 and downregulation of CD86 in circulating monocytes during early sepsis [23]. In addition, knockout of CD80 or anti-CD80 treatment conferred better survival outcomes compared to knockout of CD86 or anti-CD86 treatment in the early stage of sepsis [22]. These data imply a possible differential role for CD80 and CD86 in regulating macrophage function and implicate CD80 as a potential target for suppressing the pro-inflammatory activities of macrophages.

Macrophages are the most important source of IL-1β, a major pro-inflammatory cytokine associated with initiating inflammation. To produce IL-1β, macrophages need two signals: one through TLRs that induce gene transcription of pro-IL-1β and another through assembly of inflammasomes that cleaves biologically inactive pro-IL-1β to its active form [24]. The adaptor ASC (Pycard) is also required for assembling inflammasome complexes and an upregulation of ASC suffices to increase inflammasome activity required to generate mature, bioactive IL-1β [25]. We found that the first-responder macrophages expressed higher expression levels of ASC compared to the late responders. IL-1β and IL-23 produced from first-responder macrophages synergistically induce IL-17A production by γδT cells, which subsequently causes the adverse ventricular remodeling typical of the delayed phase after MI [13].

These heterogeneous macrophages have been conventionally classified into M_1 and M_2 macrophages based on surface marker expression.

M_1 macrophages have been implicated in tissue destruction, whereas M_2 macrophages have been implicated in wound healing and tissue repair. In line with this, the infiltrating macrophages in this study showed biphasic activation after MI, with the first-responder M_1 macrophages showing an exclusively pro-inflammatory character. However, the late-responder M_2 macrophages showed a mixed character, expressing high levels of both reparative and proinflammatory genes.

The innate immune response was followed by an adaptive immune response in the infarcted heart. This second wave of immunity could modulate the progressive ventricular remodeling that occurs late after MI. Th1 and Treg cells were the predominant subsets of $CD4^+$ T cells, whereas the Th2 and Th17 responses were minimal. As a result, a Th1/Th2 imbalance towards Th1 existed, and such a Th1/Th2 function imbalance has been associated with post-infarction cardiac insufficiency [26]. γδT cells, but not Th17 cells, are the predominant source of IL-17A in infarcted heart, while the anti-inflammatory cytokine IL-10 is produced by late-responding macrophages, regulatory T cells, DC [3], and NKT cells [27].

In the clinical setting, reperfusion therapy is performed in a substantial proportion of patients with acute MI [28]. Therefore, the impact of timely reperfusion on immune cells infiltrating the infarct area as well as the time course involved must be known. After permanent ligation, the immune response mainly depends on ischemic effects in the heart, whereas after reperfusion the response is more complex because of the additional effect of reperfusion injury. Reperfusion injury occurs during the restoration of blood flow and re-oxygenation. During ischemic periods, endothelial barrier function is thus impaired and vascular permeability increases. Restoration of blood flow into infarct-affected coronary arteries exacerbates inflammatory responses via stimulating the leakage of plasma proteins and inflammatory cells into the surrounding tissues [29]. Oxidative stress, which is generated by IR, may also induce the additional damage-associated molecular patterns (DAMPs) and prime the responsiveness of TLRs [30,31]. Although it remains unknown whether reperfusion leads to the expression of more DAMPs than ischemia and whether different signaling pathways are followed, reperfusion may activate resident cells to promote the overall inflammatory response.

The possible role of inflammation in the pathological process associated with IR injury and the impact of reperfusion on long-lasting persistent inflammation after MI should be considered separately [6,9,29]. Previous analysis of the kinetics of the inflammatory response after MI by immunohistochemistry demonstrated that reperfusion allows a faster clearance of cardiomyocyte remnants, an earlier deposition of collagen, and a stronger angiogenic response [32]. Reperfusion limits infarct volume, and we showed in the present study that the scale of global immune responses is chiefly regulated by infarct volume. Reflecting the smaller infarct size, the timely reperfusion of occluded coronary arteries reduced the total number of leukocytes accumulating in the infarcted myocardium. In addition, timely reperfusion temporally shifted the innate and adaptive immune response dynamics to an earlier point post-MI and blunted the wave of adaptive immune responses. We believe that although reperfusion therapy transiently exaggerated the acute inflammatory response in this study, it also promotes rapid clearance of DAMPs and accelerates influx and evanescence of immune cells. These findings confirmed the bank of experimental evidence indicating that timely reperfusion not only reduces inflammation in post-MI heart, but also prevents the transition from acute to persistent inflammation, and thus prevents the consequent ventricular remodeling.

Reperfusion may stimulate early inflammatory resolution beyond the golden window for myocardial salvage. In fact, previous studies reported a reduction in adverse left ventricular remodeling after late perfusion [33–35]. Contrary to this hypothesis, a randomized study involving 2166 stable patients with total occlusion of the infarct-related artery 3 to 28 days after MI and without severe inducible ischemia demonstrated that late reperfusion had no clinical benefit with respect to death and heart failure [36]. These results were remarkably consistent among patients with a low ejection fraction or an anterior MI, both of which are high risks for adverse LV remodeling. In any case, substantial changes in the immune response dynamics after MI with reperfusion should be considered when determining the optimal target and timing for immunomodulatory therapy.

5. Study limitations

The increasing number of publications on the immune response highlights the role of immune cell subsets in post-MI cardiac remodeling. For example, using an MI model with persistent total occlusion of the infarct artery, we demonstrated that activated $CD11c^+MHC^-II^+CD11b^+$ myeloid DCs have potent immunoprotective properties during the post-infarction healing process [3], whereas IL-17A-producing γδT cells exacerbate adverse remodeling [13]. If applying these experimental results in the context of immunotherapy, augmentation of DC function or suppression of γδT cell function could be expected to improve the outcomes of post-MI healing. More studies need to be carried out to better understand the mechanism of mobilization and activation of individual immune cells, cell-to-cell communications between immune cells, and the interaction between immune cells and non-immune cells, including cardiomyocytes, fibroblasts, vascular cells, and neuronal cells, all of which relate to post-MI cardiac remodeling.

Funding

This work was supported by a Grant-in-Aid for Scientific Research (KAKENHI) (to M.S.) and by PRESTO (to M.S.). Xiaoxiang Yan was supported by the Japan Society for the Promotion of Science (Postdoctoral Research Fellowships, No. 5556) and the China Scholarship Council (No. 2008623017).

Disclosures

None.

Acknowledgments

The authors thank Y. Miyake and A. Itaya for technical assistance.

Appendix A. Supplementary data

Supplementary data to this article can be found online at http://dx.doi.org/10.1016/j.yjmcc.2013.04.023.

References

[1] Krum H, Teerlink JR. Medical therapy for chronic heart failure. Lancet 2011;378:713–21.
[2] Lewis EF, Moye LA, Rouleau JL, Sacks FM, Arnold JM, Warnica JW, et al. Predictors of late development of heart failure in stable survivors of myocardial infarction: the CARE study. J Am Coll Cardiol 2003;42:1446–53.
[3] Anzai A, Anzai T, Nagai S, Maekawa Y, Naito K, Kaneko H, et al. Regulatory role of dendritic cells in postinfarction healing and left ventricular remodeling. Circulation 2012;125:1234–45.
[4] Nahrendorf M, Swirski FK, Aikawa E, Stangenberg L, Wurdinger T, Figueiredo JL, et al. The healing myocardium sequentially mobilizes two monocyte subsets with divergent and complementary functions. J Exp Med 2007;204:3037–47.
[5] Leuschner F, Rauch PJ, Ueno T, Gorbatov R, Marinelli B, Lee WW, et al. Rapid monocyte kinetics in acute myocardial infarction are sustained by extramedullary monocytopoiesis. J Exp Med 2012;209:123–37.
[6] Arslan F, de Kleijn DP, Pasterkamp G. Innate immune signaling in cardiac ischemia. Nat Rev Cardiol 2011;8:292–300.
[7] Nahrendorf M, Pittet MJ, Swirski FK. Monocytes: protagonists of infarct inflammation and repair after myocardial infarction. Circulation 2010;121:2437–45.
[8] Frangogiannis NG. Regulation of the inflammatory response in cardiac repair. Circ Res 2012;110:159–73.
[9] Marchant DJ, Boyd JH, Lin DC, Granville DJ, Garmaroudi FS, McManus BM. Inflammation in myocardial diseases. Circ Res 2012;110:126–44.
[10] Tokudome S, Sano M, Shinmura K, Matsuhashi T, Morizane S, Moriyama H, et al. Glucocorticoid protects rodent hearts from ischemia/reperfusion injury by

activating lipocalin-type prostaglandin D synthase-derived PGD2 biosynthesis. J Clin Invest 2009;119:1477–88.
[11] Shichita T, Sugiyama Y, Ooboshi H, Sugimori H, Nakagawa R, Takada I, et al. Pivotal role of cerebral interleukin-17-producing gamma delta T cells in the delayed phase of ischemic brain injury. Nat Med 2009;15:946–50.
[12] Murray PJ, Wynn TA. Protective and pathogenic functions of macrophage subsets. Nat Rev Immunol 2011;11:723–37.
[13] Yan XX, Shichita T, Katsumata Y, Matsuhashi T, Ito H, Ito K, et al. Deleterious effect of the IL-23/IL-17A axis and γδT cells on left ventricular remodeling after myocardial infarction. J Am Heart Assoc 2012;1:e004408. http://dx.doi.org/10.1161/JAHA.112.
[14] Joiner ML, Koval OM, Li J, He BJ, Allamargot C, Gao Z, et al. CaMKII determines mitochondrial stress responses in heart. Nature 2012;491:269–73.
[15] Li J, Horak KM, Su H, Sanbe A, Robbins J, Wang X. Enhancement of proteasomal function protects against cardiac proteinopathy and ischemia/reperfusion injury in mice. J Clin Invest 2011;121:3689–700.
[16] Nagoshi T, Matsui T, Aoyama T, Leri A, Anversa P, Li L, et al. PI3K rescues the detrimental effects of chronic Akt activation in the heart during ischemia/reperfusion injury. J Clin Invest 2005;115:2128–38.
[17] Narayan N, Lee IH, Borenstein R, Sun J, Wong R, Tong G, et al. The NAD-dependent deacetylase SIRT2 is required for programmed necrosis. Nature 2012;492:199–204.
[18] Xiang SY, Vanhoutte D, Del Re DP, Purcell NH, Ling H, Banerjee I, et al. RhoA protects the mouse heart against ischemia/reperfusion injury. J Clin Invest 2011;121:3269–76.
[19] Fujiu K, Manabe I, Nagai R. Renal collecting duct epithelial cells regulate inflammation in tubulointerstitial damage in mice. J Clin Invest 2011;121:3425–41.
[20] Altwegg LA, Neidhart M, Hersberger M, Muller S, Eberli FR, Corti R, et al. Myeloid-related protein 8/14 complex is released by monocytes and granulocytes at the site of coronary occlusion: a novel, early, and sensitive marker of acute coronary syndromes. Eur Heart J 2007;28:941–8.
[21] Ionita MG, Vink A, Dijke IE, Laman JD, Peeters W, van der Kraak PH, et al. High levels of myeloid-related protein 14 in human atherosclerotic plaques correlate with the characteristics of rupture-prone lesions. Arterioscler Thromb Vasc Biol 2009;29:1220–7.
[22] Nolan A, Kobayashi H, Naveed B, Kelly A, Hoshino Y, Hoshino S, et al. Differential role for CD80 and CD86 in the regulation of the innate immune response in murine polymicrobial sepsis. PLoS One 2009;4:e6600.
[23] Nolan A, Weiden M, Kelly A, Hoshino Y, Hoshino S, Mehta N, et al. CD40 and CD80/86 act synergistically to regulate inflammation and mortality in polymicrobial sepsis. Am J Respir Crit Care Med 2008;177:301–8.
[24] Schroder K, Tschopp J. The inflammasomes. Cell 2010;140:821–32.
[25] Gavrilin MA, Abdelaziz DH, Mostafa M, Abdulrahman BA, Grandhi J, Akhter A, et al. Activation of the pyrin inflammasome by intracellular *Burkholderia cenocepacia*. J Immunol 2012;188:3469–77.
[26] Cheng X, Liao YH, Ge H, Li B, Zhang J, Yuan J, et al. TH1/TH2 functional imbalance after acute myocardial infarction: coronary arterial inflammation or myocardial inflammation. J Clin Immunol 2005;25:246–53.
[27] Sobirin MA, Kinugawa S, Takahashi M, Fukushima A, Homma T, Ono T, et al. The activation of natural killer T cells ameliorates post-infarct cardiac remodeling and failure in mice. Circ Res 2012.
[28] Kushner FG, Hand M, Smith Jr SC, King III SB, Anderson JL, Antman EM, et al. 2009 focused updates: ACC/AHA guidelines for the management of patients with ST-elevation myocardial infarction (updating the 2004 guideline and 2007 focused update) and ACC/AHA/SCAI guidelines on percutaneous coronary intervention (updating the 2005 guideline and 2007 focused update): a report of the American College of Cardiology Foundation/American Heart Association Task Force on Practice Guidelines. Circulation 2009;120:2271–306.
[29] Eltzschig HK, Eckle T. Ischemia and reperfusion—from mechanism to translation. Nat Med 2011;17:1391–401.
[30] Powers KA, Szaszi K, Khadaroo RG, Tawadros PS, Marshall JC, Kapus A, et al. Oxidative stress generated by hemorrhagic shock recruits Toll-like receptor 4 to the plasma membrane in macrophages. J Exp Med 2006;203:1951–61.
[31] Gill R, Tsung A, Billiar T. Linking oxidative stress to inflammation: Toll-like receptors. Free Radic Biol Med 2010;48:1121–32.
[32] Vandervelde S, van Amerongen MJ, Tio RA, Petersen AH, van Luyn MJ, Harmsen MC. Increased inflammatory response and neovascularization in reperfused vs. non-reperfused murine myocardial infarction. Cardiovasc Pathol 2006;15:83–90.
[33] Piscione F, Galasso G, De Luca G, Marrazzo G, Sarno G, Viola O, et al. Late reopening of an occluded infarct related artery improves left ventricular function and long term clinical outcome. Heart 2005;91:646–51.
[34] Horie H, Takahashi M, Minai K, Izumi M, Takaoka A, Nozawa M, et al. Long-term beneficial effect of late reperfusion for acute anterior myocardial infarction with percutaneous transluminal coronary angioplasty. Circulation 1998;98:2377–82.
[35] Appleton DL, Abbate A, Biondi-Zoccai GG. Late percutaneous coronary intervention for the totally occluded infarct-related artery: a meta-analysis of the effects on cardiac function and remodeling. Catheter Cardiovasc Interv 2008;71:772–81.
[36] Hochman JS, Lamas GA, Buller CE, Dzavik V, Reynolds HR, Abramsky SJ, et al. Coronary intervention for persistent occlusion after myocardial infarction. N Engl J Med 2006;355:2395–407.